Fusion of the most neutron-rich nucleus 8He : Recent results from GANIL

A. Lemasson

EPJ Web of Conferences **17**, 01003 (2011)
DOI: 10.1051/epjconf/20111701003

Fusion of the most neutron-rich nucleus ^{8}He: Recent results from GANIL

A. Lemasson[1,2,a]

[1] NSCL, Michigan State University, East Lansing, MI 48824, USA
[2] GANIL, CEA/DSM - CNRS/IN2P3, Bd Henri Becquerel, BP 55027, F-14076 Caen Cedex 5, France

Abstract. Re-accelerated radioactive ions beams of ^{8}He from the SPIRAL facility at GANIL have been used to perform the first experimental investigations at energies around the Coulomb barrier of fusion and direct reactions with the most neutron rich ^{8}He. Two experiments (in the ^{8}He+^{65}Cu and ^{8}He+^{197}Au systems) have been performed, using the complementarity of in-beam and off-beam techniques, to measure integral and differential cross sections for elastic scattering, fusion and neutron(s) transfer. These results, compared with Coupled Reaction Channels calculations as well as phenomenological approaches allowed to probe and understand the different facets of the interplay between the intrinsic structure of ^{8}He and reaction mechanisms.

1 Introduction

Recent advances in accelerator and isotope-production technology, like the Isotope Separation On-Line (ISOL) technique, provides new opportunities to study and understand reactions involving rare short-lived isotopes [1–4]. These nuclei far from the β-stability line, characterised by small binding energies and unusual ratio of neutron to proton numbers, have a variety of novel properties like extended and therefore diluted matter distributions (halo), Borromean structures (three-body bound systems, where any of its two-body subsystems are unbound) or large breakup probabilities. Theses new intrinsic properties, that differs significantly from those of stable nuclei, are expected to influence reaction mechanisms at energies around the Coulomb barrier and are also relevant to reactions of astrophysical interest [5]. The large probability of breakup associated with the weak binding of the valence nucleon(s) led to the expectation that breakup of the projectile would be a dominant channel and also influence the reaction mechanism for these nuclei [1–3]. Attempts have been made to understand the influence of the breakup process on the fusion and elastic scattering of beams of both stable and radioactive weakly bound nuclei using various approaches. However, the loosely bound valence nucleon(s) could also imply large transfer cross sections from the projectile to the target. This in turn would also be expected to influence the reaction mechanism. In particular, Borromean nuclei (in which the binding is essentially arising from pairing correlations) represents a unique tool to understand the dynamical aspects of pairing correlations between loosely bound nucleons through the study of the relative importance of $1n$ and $2n$ transfer [6,7].

In this talk we present the first investigations of reaction mechanisms at energies around the Coulomb barrier involving the ^{8}He nucleus. The heaviest Helium isotope, with the largest neutron/proton ratio (3/1) of known bound nuclei and a lifetime of only 0.12 s, is a weakly-bound nucleus (S_{2n} = 2.1 MeV) exhibiting an neutron halo/skin and a Borromean structure. The increase of the two neutron separation energy (S_{2n}) in the more neutron-rich ^{8}He compared to ^{6}He is different from the known behavior for other isotopic chains. The helium isotopic chain, where the neutron emission threshold varies from 20.5 MeV to 0.9 MeV, represents an ideal laboratory for studying the effect of the weak binding and of the changing intrinsic structure with increasing number of neutrons on reaction mechanisms. Moreover, if Helium isotopes are considered as composite objects of interacting (α core) and non interacting (valence neutrons) objects with respect to the electrostatic barrier, the fusion reaction of Helium isotopes can be seen as a ideal case for studying the quantum tunnelling of composite objects [8,9].

The SPIRAL facility at GANIL provides the most intense beams of ^{8}He presently available, giving a unique opportunity to study neutron correlations and the effect of Borromean structure on the reaction mechanisms at energies around the Coulomb barrier. However, measurements with low intensity ($\sim 10^{5}$ pps) and low energy re-accelerated beams of rare short-lived isotopes represent an experimental challenge due to the million time lower intensity compared to stable beams. Hence, the development of innovative sensitive and selective methods is required to reach new mea-

[a] e-mail: lemasson@nscl.msu.edu

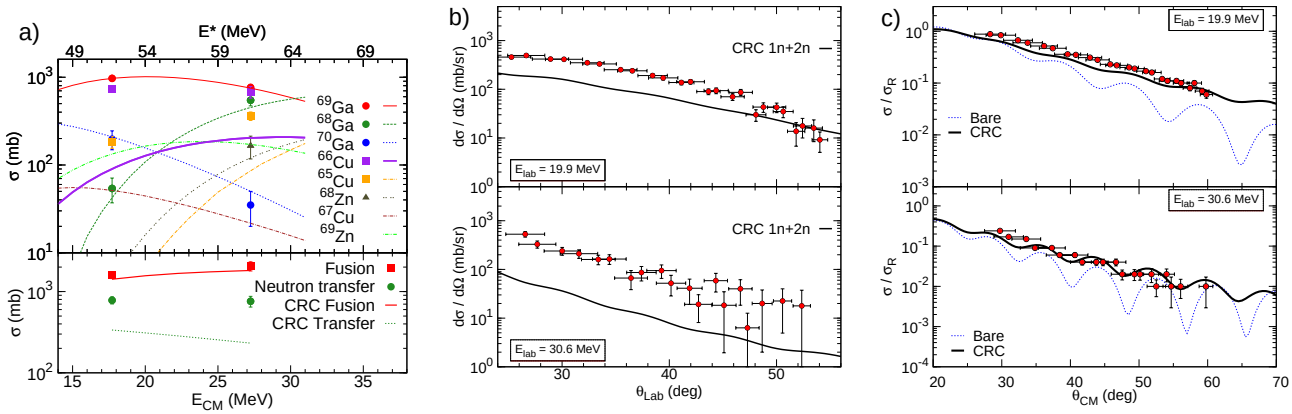

Fig. 1. (a) Heavy residue, fusion, and neutron- transfer excitation functions for the ^{8}He+^{65}Cu system: (upper panel) Measured partial residue cross sections as a function of the center-of-mass energy. The lines are obtained using the statistical model code CASCADE. (lower panel) Fusion and neutron-transfer cross sections for the ^{8}He+^{65}Cu system. Predictions from Coupled Reaction Channels calculations for fusion (continuous lines) and neutron transfer (dashed lines) are also shown. (b) 1n+2n transfer angular distributions at E_{lab} = 19.9 MeV (upper panel) 30.6 MeV (lower panel) along with corresponding CRC calculations for $1n + 2n$ transfer. (c) Elastic-scattering angular distributions obtained at E_{lab} = 19.9 MeV (upper panel) and 30.6 MeV (lower panel) along with no-coupling (bare) calculations (dotted line) and CRC calculations including couplings to 1n and 2n transfer (full line).

surement limits and also to measure and disentangle the different reaction processes.

With the above motivations, two independent experiments were performed with low intensity radioactive ions beams of ^{8}He. The complementarity of *in-beam* and *off-beam* sensitive and selective experimental techniques was used to obtain integral and differential cross sections for elastic scattering, neutron(s) transfer and fusion of the ^{8}He projectile on two different targets. These various experimental results combined with Coupled Reaction Channels calculations and with a phenomenological analysis, represent a significant step toward a consistent understanding of reaction mechanisms with ^{8}He at energies around the Coulomb barrier. These different aspects of the talk are presented in the following sections. First, the experimental results for ^{8}He+^{65}Cu and ^{8}He+^{197}Au systems are presented respectively in the section Sect. 2.1 and 2.2. A discussion of these results is presented in Sect. 3 using Coupled Reaction Channels calculations and a systematic study of fusion and transfer excitation functions in the Helium isotopic chain.

2 Recent experimental investigations with ^{8}He at GANIL SPIRAL facility

Radioactive ion beams of ^{8}He were produced by fragmentation of a 75 MeV/nucleon ^{13}C beam on a thick graphite target, then fully purified and re-accelerated by the CIME cyclotron at the SPIRAL facility at GANIL. The ^{8}He beam, with an energy resolution better than 2×10^{-3}, a beam spot size of $\sim$ 5 mm diameter and an average intensity of $(2-4)\times10^{5}$ particles/s. Two experiments were performed in the ^{8}He+^{65}Cu and ^{8}He+^{197}Au employing two independent setups respectively using in-beam and off-beam techniques are presented in the following paragraphs.

2.1 Complete reaction studies above the Coulomb barrier in the ^{8}He+^{65}Cu system

Reaction mechanisms with ^{8}He were investigated by means of *in-beam* measurements performed in the ^{8}He + ^{65}Cu system [10]. This experiment aimed at the simultaneous measurement of fusion and direct reactions (elastic scattering and neutron(s) transfer) at energies above the Coulomb barrier. Simultaneously, the goal was to improve the sensitivity of in-beam measurements with low-intensity ISOL beams. The experimental setup consisted of 12 Compton suppressed Clover γ-ray detectors (EXOGAM array), a Silicon stripped ΔE-E annular detector and 45 neutron detectors (Neutron Wall array). At two beam energies (19.9 and 30.6 MeV), inclusive and exclusive measurements of γ-rays from target-like residues, charged particles (^{4,6,8}He) and neutrons were used to obtain integral fusion and neutron(s) transfer cross sections as well as differential cross sections for elastic scattering and neutron(s) transfer.

The individual residue cross sections were obtained using the corresponding intensities of the well-known, low-lying γ transitions from the measured inclusive γ-ray spectra. Figure 1(a) shows the residue cross sections as a function of the center-of-mass energy for the ^{8}He+^{65}Cu system. The lines in the figure are the results of statistical model calculations for the evaporation residues formed in the decay of ^{73}Ga using the statistical model code CASCADE [11]. As can be

seen from the figure, the various partial cross sections are reasonably well explained by the statistical model except for the $\alpha 3n$ and $\alpha 4n$ evaporation channels (^{66}Cu and ^{65}Cu residues, respectively). Such a discrepancy between the measured and calculated cross sections for ^{66,65}Cu was observed earlier in the case of ^{6}He+ ^{65}Cu [12], and was shown to arise from neutron(s)-transfer processes. The total fusion cross sections were then obtained from the sum of the individual evaporation cross sections for ^{68,69,70}Ga and ^{68}Zn and corrected for the ^{65,66}Cu and ^{69}Zn contributions using the CASCADE statistical model calculation. Similarly, the integral neutron-transfer cross sections were obtained from the measured intensities of the inclusive γ-ray spectra of ^{65,66}Cu after correcting for compound nucleus contributions and the total cross sections are shown in Fig. 1(a).

Exclusive measurements of γ rays in coincidence with light charged particles have been used to further characterize the direct reactions induced by this double-Borromean nucleus. Due to the large positive Q-values for 2n transfer (Q = 14.0 MeV) and the Borromean nature of ^{8}He, the direct measurement of individual $1n$ and $2n$ transfer cross sections from the observed final residues after one- and two-neutron transfer to heavy targets is not possible in the present case, since the residues are the same in both reaction channels. The $(1n+2n)$ transfer differential cross sections were obtained from exclusive measurements of charged particles (^{4,6}He) and γ-rays from heavy transfer residues (so as to separate neutron(s) transfer from break-up process) and are shown in Fig. 1(b). Upper limits on projectile breakup differential cross sections were estimated from the difference between inclusive and exclusive charged particles angular distributions, suggesting that their amplitude is smaller that those obtained for neutron(s) transfer (contrary to simple expectations). Triple coincidences between γ-rays, charged particles and neutrons were also measured with this low intensity beam. Despite having the most intense ^{8}He beam available today at GANIL, it was not possible to determine individual cross sections for $1n$ and $2n$ transfer using kinematic correlation of energies and emission angles between ^{6}He particles and neutrons in coincidence with γ-rays (a method used earlier with 200 times more intense ^{6}He beams [6]). However, an alternative approach to obtain lower limit on ratio of $2n$ to $1n$ transfer cross sections using integral cross sections measured in the ^{8}He+^{197}Au system is discussed in the next section.

The elastic scattering angular distributions of ^{8}He in the laboratory angular range between 25° and 60° at 19.9 and 30.6 MeV were obtained with inclusive measurements of ^{8}He and are shown in Fig 1(c).

This study in the ^{8}He+^{65}Cu system represents the most complete study of compound and direct reactions induced by ^{8}He at energies above the Coulomb barrier using in-beam measurements. The feasibility of measuring absolute cross sections using inclusive in-beam γ-ray measurements with $\sim 10^5$ pps ISOL radioactive beams has been demonstrated. Such measurements have been made possible owing to very good beam quality in conjunction with highly efficient detector systems and open new possibilities for in-beam reaction studies with low-intensity RIB at present and future facilities.

2.2 Sub-barrier fusion and transfer in the ^{8}He+^{197}Au system

In order to further probe the reaction mechanisms with ^{8}He using another target and address the question of the behaviour of fusion cross sections at sub-barrier energies, an off-beam experiment was performed in the ^{8}He+^{197}Au system [16]. ^{8}He beams were used to bombard a stack of ^{197}Au targets. The target stacks consisted of two or three Au targets ($\sim$ 6 mg/cm^2 thick) separated by Al foils ($\sim$ 1 mg/cm^2 thick) to collect recoiling residues and Al foils (from 2 to 10 mg/cm^2 thick) to degrade the beam energy. The different target stacks were irradiated at energies of 2.34, 2.51 and 3.68 MeV/nucleon for 150 h, 24 h and 32 h, respectively. The intensity of the ^{8}He beam was measured using a microchannel plate and a plastic scintillator ($10 \times 10 \times 0.05$ cm) placed, respectively, 10 cm upstream and 5 cm downstream with respect to the target. Their time-stamped energy and time signals, correlated with the cyclotron frequency, were used to measure the ^{8}He beam intensity and its time variation during the irradiation. The ^{199,202}Tl nuclei, arising after the evaporation of neutrons from the compound nucleus ^{205}Tl, were characterized by their radioactive decay. These off-beam measurements were made using two lead-shielded detector setups, the first optimized for X-γ coincidences and the second consisting of two clover detectors to maximize the X-ray detection efficiency. Absolute photo-peak efficiencies of the above two setups were obtained using complete GEANT4 [17] simulations which reproduced within 4% the results of measurements made with five calibration sources (including a ^{201}Tl source) at various distances. Unambiguous identification of the energy and time of disintegration was obtained using a new sensitive and accurate off-beam coincidence technique specialized for the measurement of absolute evaporation residue cross sections involving low intensity RIB. This method, applied earlier to high intensity stable beams [14], involves the simultaneous measurement of X and γ rays emitted in electron capture decays. The final gain in sensitivity, compared to an inclusive experiment, was found to be $\sim$ 30000, yielding the first complete and most accurate (having the same quality as for stable beams) fusion cross sections measured with re-accelerated RIB. The smallest cross sections measured here (Fig. 2(a)) using re-accelerated RIB are comparable to the current measurement limits in nuclear physics, when scaled by the million times larger intensities available with stable beams. Shown in Fig. 2(a) are the measured individual fusion evapo-

ration residue cross sections, ER, as a function of the excitation energy together with predictions of Bohr's model of the statistical decay of an equilibrated compound nucleus [11]. The excellent agreement between the measured ER and the calculations confirms that the residues arise from the complete fusion of ^{8}He and ^{197}Au. The fusion cross section, σ_F, obtained from the sum of the ER, is shown in Fig. 2(b). The residues formed after transfer of neutron(s) from the projectile (isotopes of gold) were identified and their activity obtained using inclusive γ-ray measurements. The total transfer cross section, obtained from the sum of the cross sections for ^{198,198m,199}Au, residues is also shown.

The experimental investigations in the ^{8}He+^{65}Cu system showed that it was not possible to obtain individual differential cross sections for $1n$- and $2n$- transfer not only due to the low beam intensity, but also due to the complex structure of ^{8}He, suggesting that alternative experimental approaches were required. The off-beam measurements in the ^{8}He+^{197}Au system unexpectedly revealed significant cross sections for the $2n$ transfer residue ^{199}Au in the ^{8}He+^{197}Au system (as compared to the non-observation of the ^{67}Cu residue in the ^{8}He+^{65}Cu system). This observation gave an unique opportunity to derive from these integral cross sections a lower limit on the ratio of two- and one-neutron transfer cross sections (σ_{2n}/σ_{1n}) for ^{8}He [15]. The difference of the survival probability between $2n$ transfer residues ^{67}Cu and ^{199}Au was qualitatively explained using simple calculations of the density of $2n$ states populated in target-like nuclei in two neutrons transfer. A lower limit of $\sigma_{2n}/\sigma_{1n} > 0.3$ was obtained, representing a first constrain for reaction models in order to understand the role of pairing correlations between loosely bound nucleons in ^{8}He.

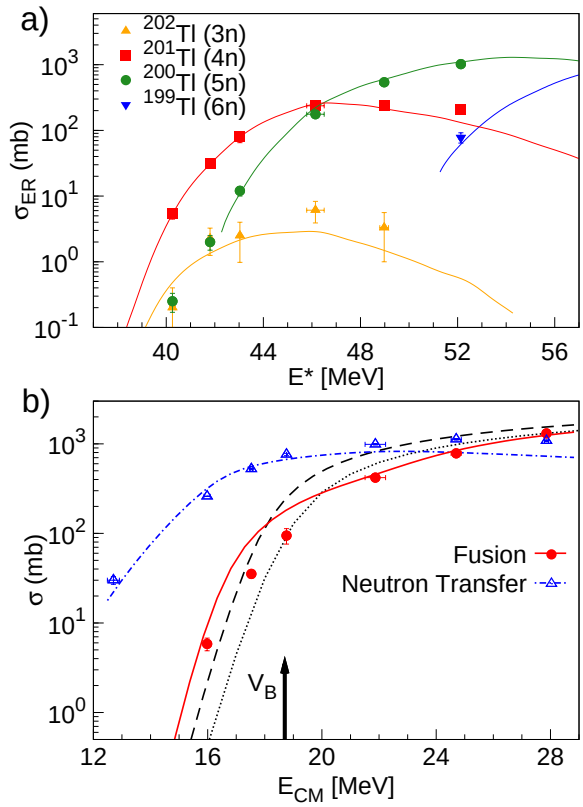

Fig. 2. (a) Cross sections for evaporation residues as a function of excitation energy of the compound nucleus in the ^{8}He+^{197}Au. The lines correspond to predictions based on the statistical model code CASCADE. (b) Fusion and neutron transfer excitation functions for the ^{8}He+^{197}Au. Two predictions for fusion based on tunneling through a single barrier depending only on the radial separation are shown; dotted line using a nuclear potential derived from a global parametrization [20]; dashed line using a microscopic potential folding the nuclear densities of the target and the projectile. The coupled-channels calculations for fusion and transfer reactions are shown by continuous and dash-dotted lines, respectively. The nominal value of the Coulomb barrier (V_B) is indicated.

3 Results and Discussion

3.1 Comparison with CRC calculations

The experimental results obtained for ^{8}He+^{65}Cu and ^{8}He+^{197}Au systems were compared to Coupled Reaction Channels (CRC) calculations to understand the inter-connectivity between the compound and direct reactions in the reactions induced by ^{8}He at energies around the Coulomb Barrier. These calculations using the code FRESCO [18] included realistic double-folded potentials (that take into account the spatial extension of the neutron distribution) and coupling to 1n and 2n transfer channels as direct, one step processes.

The excitation function for fusion and neutron transfer obtained in the ^{8}He+^{197}Au system are shown in Fig. 2(b) along with calculations. The calculated fusion cross sections for tunneling through a single barrier, depending only on the internuclear distance, calculated with a nuclear potential derived either from a global parametrization [20] (dotted) or from a microscopic double-folded potential using realistic densities (dashed). The difference between the two calculations demonstrates the effect of the extended neutron distribution of the ^{8}He nucleus. The dramatic decrease in the measured fusion cross section for energies at and above the barrier, along with a modest increase below the barrier (with respect to the dashed line) can be observed from the figure. The dominance of the transfer processes is seen from the magnitude of the measured transfer cross sections that are much larger than fusion cross sections even at energies well above the barrier. CRC calculations are also presented on the figure (more details on the calculations can be found in Ref. [16]). The observed behavior of the fusion excitation function is reproduced by the CRC calculations (continuous line) including coupling to the transfer channels (dash-dotted line). The good agreement of

the calculations including only neutron transfer channels shows that the low particle threshold (2.1 MeV) does not imply a crucial influence of breakup of the projectile on the tunneling process, as is generally assumed for weakly bound nuclei. The cross sections both below and above the barrier for fusion and neutron(s) transfer were simultaneously very well reproduced suggesting that the main processes were included the calculations. The very large cross sections observed for neutron(s) transfer (larger than fusion, even at energies above the Coulomb barrier) seems to be, at the present date, a unique feature of the ^{6,8}He isotopes highlighting the pre-dominant role of neutron transfer for these neutron rich weakly bound projectiles. Despite these very large cross sections observed for neutron(s) transfer, only a modest enhancement of the fusion cross section of ^{8}He on ^{197}Au at energies below the Coulomb barrier was observed with respect to conventional 1D barrier penetration model.

In the ^{8}He+^{65}Cu system, the influence of neutron(s) transfer in reaction involving ^{8}He were further investigated by comparing similar CRC calculations to differential cross sections (for elastic scattering and neutron(s) transfer) as well as integral cross sections (for fusion an neutron(s) transfer). The CRC calculations are presented in the Fig. 1 along with the different observables. For the $1n + 2n$ transfer, a qualitative agreement between experimental observations and calculations is obtained for the shape of angular distributions (Fig. 1(b)) but the amplitude of the cross sections is underestimated for the sum of $1n + 2n$ transfer cross sections. Consistently, the integral cross sections for neutrons transfer are underestimated (Fig. 1(a), lower panel). This suggests that other reaction mechanisms such as sequential transfer of two neutrons could also contribute to the total transfer cross sections. Nevertheless, the calculations show that the coupling to $1n$ and $2n$ transfer channels has a significant influence on elastic scattering (Fig. 1 (c)), and this despite the energies being much above the Coulomb barrier ($E/V_B = 2.3$ and 3.4) (more details on the CRC calculations can be found in Ref. [10]). The structural complexity of ^{8}He (a 5-body object) represents a challenge for future reaction models and more realistic calculations cannot be preformed at the present date.

However, theses comparisons between CRC calculations including coupling to one- and two- neutron transfer channels and the different observables measured in two systems gave a consistent description of the reactions at energies around the Coulomb barrier involving the neutron rich nucleus ^{8}He. These results highlight the influence of the specific structure of ^{8}He on the reaction mechanisms: the extra valence neutrons lead to a dominance of transfer reactions, and this dominance continues up to much higher energies than would be inferred by extrapolating studies with stable nuclei.

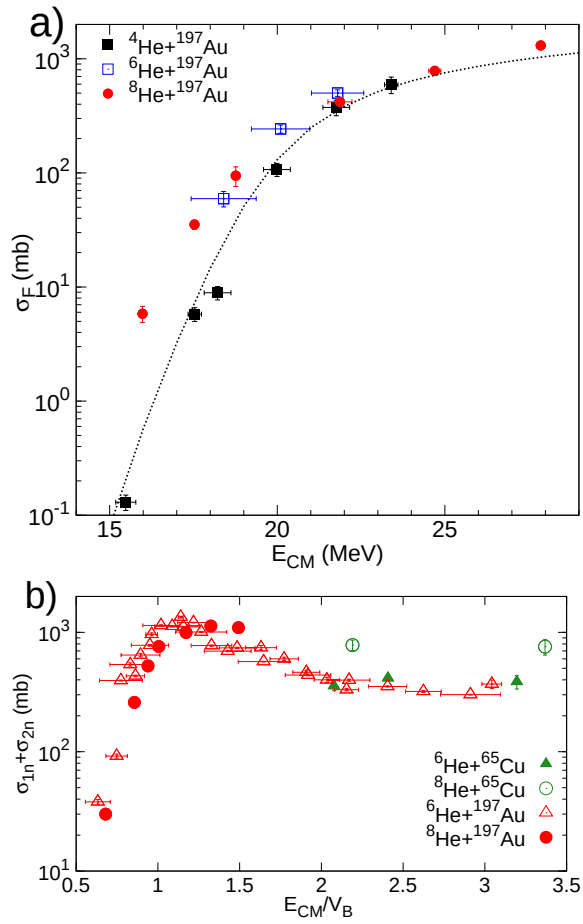

Fig. 3. (a) Measured fusion cross section as a function of center-of-mass energy (E_{CM}) for ^{4,6,8}He+^{197}Au systems. The data for ^{6,8}He+^{197}Au systems are from Refs. [21, 13]. The dotted line shows the one-dimensional barrier penetration calculation for ^{4}He+^{197}Au obtained using a global parametrization for the nuclear potential. (b) Measured total neutron transfer cross sections ($\sigma_{1n} + \sigma_{2n}$) for ^{6,8}He+^{65}Cu [6,12,10] and ^{6,8}He+^{197}Au [13,10] systems as function of the center-of-mass energy energy normalized by the Coulomb barrier of the system.

3.2 Model independent study in the Helium isotopic chain

Beyond the comparison with reaction models, experimental results can also be discussed in a model independent way. Figure 3(a) shows the measured fusion cross sections for helium isotopes with ^{197}Au. The good agreement between the calculated and measured fusion cross section for ^{4}He reiterates its point like behavior. At energies below the barrier, the fusion cross sections for ^{8}He and ^{6}He are as expected larger than for ^{4}He, but show an unusual behaviour: the addition of a neutron pair to ^{6}He did not increase the probability of fusion, contrary to the increase found in going from ^{4}He to ^{6}He and that usually observed with increasing masses in other isotopic chains. Loosely bound systems, like ^{6,8}He, with va-

lence neutrons that does not feel the barrier can more easily restructure during the dynamical process of fusion, emphasizing the role of a flexible intrinsic wave function that can adiabatically readjust in a slow process and increase penetration. For a loosely bound but essentially isotropic system like ^{8}He, it turns out to be easier to transfer part of the neutron excess to the target than to readjust the outer skin of the system, tunnel as a whole and fuse. The observed similarity of the low-energy results for ^{8}He and ^{6}He may indicate the role of higher order processes with neutron-pair transfer preceding fusion. To exemplify the role of the neutron pairs in the Borromean nuclei ^{6,8}He, the sum $\sigma_{1n} + \sigma_{2n}$ is shown in Fig. 3(b) as a function of energy normalized to the Coulomb barrier. The total transfer cross sections have a similar trend for both targets. At energies around the barrier the cross sections are comparable while above the barrier they are larger for ^{8}He. The observed difference between ^{6}He and ^{8}He on both targets can be attributed to the structure of the projectile. Earlier studies on proton targets showed that ^{8}He cannot be considered just as an inert α core plus 4 neutrons; excited states of ^{6}He are populated with significant probability [24] confirming the role of core excitations in the formation of Cooper pairs [25]; Ref. [7] suggests that pairing can be supported by coupling to the phonon-like excitations of the core, in this specific case to the 2^{+} state in ^{6}He. The larger cross section seen for ^{8}He compared to ^{6}He at higher energy may reflect a considerable difference in geometry of valence neutrons in these isotopes. Dynamics of such processes with loosely bound neutrons should be a subject of deeper theoretical studies.

4 Summary and Conclusion

In conclusion, re-accelerated radioactive ions beams of ^{8}He from the SPIRAL facility have been used to perform the first experimental investigations at energies around the Coulomb barrier of fusion and direct reactions with the most neutron rich nucleus ^{8}He. These results could only be obtained due the development of a sensitive, selective and accurate off-beam technique to measure absolute cross sections and the high quality of the re-accelerated beams. Two experiments (in the ^{8}He+^{65}Cu and ^{8}He+^{197}Au systems) have been performed, using the complementarity of in-beam and off-beam techniques, to measure integral and differential cross sections of elastic scattering, fusion and neutron(s) transfer. These results combined with reaction models as well as a phenomenological approach allowed to probe and understand the different features of the interplay between the intrinsic structure of ^{8}He and reaction mechanisms, highlighting the predominant role of neutron(s) transfer in the reactions involving neutron-rich helium isotopes. Next generation facilities, like SPIRAL2, with high quality and intensity re-accelerated radioactive ion beams, represent unique tools to reveal and further probe with unprecedent accuracy new facets of reaction mechanisms involving rare isotopes nuclei at energies around the Coulomb barrier.

Acknowledgements

The author would like to thank all the collaborators that have contributed to the different parts of the work that have been presented in this manuscript.

References

1. L. Canto, P. Gomes, R. Donangelo, and M. Hussein, Phys. Rep. **424**, 1 (2006).
2. N. Keeley, N. Alamanos, K. Kemper and K.Rusek, Prog. Part. Nucl. Phys. **63**, 396 (2009).
3. N. Keeley, R. Raabe, N. Alamanos, and J. L. Sida, Prog. Part. Nucl. Phys. **59**, 579 (2007).
4. A. Navin, F. De Oliveira, P. Roussel-Chomaz, and O. Sorlin, J. Phys. G **38**, 024004 (2011).
5. I. Thompson and F. Nunes, *Nuclear Reactions for Astrophysics* (Cambridge University Press, Cambridge, 2009).
6. A. Chatterjee *et al.*, Phys. Rev. Lett. **101**, 032701 (2008).
7. G. Potel, et al., Phys. Rev. Lett. **105**, 172502 (2010); G. Potel in these proceedings.
8. C. A. Bertulani, V. V. Flambaum and V. G. Zelevinsky J. Phys. G. **34**, 2289 (2007).
9. N. Ahsan and A. Volya. Phys. Rev. C.**82**, 8 (2010).
10. A. Lemasson *et al.*, Phys. Rev. C **82**, 044617 (2010).
11. F. Pühlhofer, Nucl. Phys. A **280**, 267 (1977).
12. A. Navin *et al.*, Phys. Rev. C **70**, 44601 (2004).
13. Yu.E. Penionzhkevich et al., Eur. Phys. J. A **31**, 185 (2007).
14. A. Lemasson *et al.*, Nucl. Instr. Meth., A **598**, 445 (2009).
15. A. Lemasson *et al.*, Phys. Lett. B **697**, 454 (2011).
16. A. Lemasson *et al.*, Phys. Rev. Lett. **103**, 032701 (2009).
17. S. Agostinelli et al., Nucl. Instrum. Methods Phys. Res., Sect. A **506**, 250 (2003).
18. I. J. Thomson, Comput. Phys. Rep. **7**, 167 (1988).
19. L. F. Canto et al., J. Phys. G **36**, 015109 (2009).
20. O. Akyüz and A.Winther, Proceedings of the Enrico Fermi International School of Physics 1979 (North-Holland, Amsterdam, 1981).
21. M. S. Basunia, H. A. Shugart, A. R. Smith, and E. B. Norman, Phys. Rev. C **75**, 015802 (2007).
22. Y. Aritomo, Phys. Rev. C **75**, 024602 (2007).
23. N. D. Antunes, F. C. Lombardo, D. Monteoliva, and P. I. Villar, Phys. Rev. E **73**, 066105 (2006).
24. N. Keeley, et al., Phys. Lett. B **646**, 222 (2007).
25. W. von Oertzen, A. Vitturi, Rep. Prog. Phys. **64**, 1247 (2001).